Outage Probability of Correlated RIS-Aided Communication Links

Outage Probability of Correlated RIS-Aided Communication Links

Giorgio Taricco
Politecnico di Torino – DET, Torino Italy
E-mail: taricco@polito.it

***Abstract*—A second-order approximation of the Moment-Generating Function (MGF) for the sum of the product of correlated Rayleigh envelopes (a well-known problem in the literature) is presented in this paper. The MGF is applied to evaluate the outage probability of Reconfigurable Intelligent Surfaces (RIS) in both uncorrelated and correlated environments. Key contributions include the derivation of the MGF approximation and its application to outage probability assessment in different scenarios. The accuracy of the approximation is analyzed under two distinct correlation conditions, demonstrating its reliability in providing outage probability estimates. The results emphasize the effectiveness of the approximation as a practical tool for evaluating the outage probability in RIS-based systems, especially in correlated environments. These findings offer valuable insights for future research and practical implementations of RIS in wireless communication systems, particularly in optimizing system performance in the presence of varying correlation conditions.**

***Index Terms*—5G, 6G, Reconfigurable Intelligent Surfaces, Outage Probability, Block Fading Channels.**

I. Introduction

As noticed in [1], the term Reconfigurable Intelligent Surface (RIS) encompasses any surface that can be configured to interact with the incoming electromagnetic field in order to synthesize the scattering and absorption properties of other objects [2]. The purpose of the RIS technology is improving the characteristics of the radio link between transmitters and receivers with limited channel quality. The RIS technology can be implemented by using metasurfaces consisting of several sub-wavelength-sized passive reflecting elements (REs) [3]. The REs act like nearly isotropic scatterers and can be adjusted by using a microcontroller to steer the incident electromagnetic signals into the desired direction. The goal of RIS technology is providing ubiquitous access to high-rate communications to existing and forthcoming cellular networks, in particular within the framework of Sixth-Generation (6G) networks. Many recent applications, like enhanced Mobile BroadBand (eMBB), Ultra-Reliable, Low Latency Communications (URLLC), and massive Machine-Type Communications (mMTC) (characteristic of Fifth-Generation (5G) communication systems) are expected to benefit from RIS. Even more 6G systems encompassing data-driven, instantaneous, ultra-massive, and ubiquitous wireless connectivity [4], [5].

RIS's are credited for a large number of potential advantages, like deployment simplicity, improved spectral efficiency (which is the focus of this work), environmental friendliness (since they are mostly made of passive elements), and compatibility with existing wireless communication standards and devices [5]. Their implementation can be based on different technologies, including waveguide-fed metasurfaces, refracting and reflecting metasurfaces, and purely reflecting metasurfaces based on varactor diodes with a tunable biasing voltage. The theoretical physical foundations of RIS metasurfaces are based on Love's field equivalence principle, which states that the electromagnetic field on a closed surface is determined by the electric and magnetic currents on the surface [6]. Therefore, the management of metasurfaces can be handled by a microcontroller which injects currents in the REs in order to steer the radiation pattern in the desired direction.

The performance limits of RIS's have been studied extensively but are not yet fully understood [5]. The channel model is quite complex and therefore the information theoretical analysis aimed at discovering the achievable rate is difficult. Most of the literature resorts to approximations, which are sometimes coarse. This work focuses on the single-antenna transmitter and receiver system aided by an RIS with an array of REs. This model has been proposed in [1] and is based on a *rich scattering* assumption and the isotropic scattering assumption on the REs. It leads to Rayleigh distributed channel gains from the transmitter to the receiver, the transmitter to the RIS, and the RIS to the receiver. A major contribution of [1] is the assessment of the correlation structure of the gains from the transmitter to the RIS and the RIS to the receiver. The following contributions are presented in this paper.

- A second-order approximation of the Moment-Generating Function of the sum of the product of correlated Rayleigh envelopes (see [7], [8] for additional information).
- The application of the previous approximation for the evaluation of the outage probability of an uncorrelated or correlated RIS.

A. Organization

The paper is organized as follows. Section II characterizes the RIS considered by the definition of its parameters, it introduces the outage probability and its derivation from the MGF. Section III provides an analytic derivation of the MGF leading to an exact formula in the uncorrelated case and to a second-order approximation in the correlated case. Section III-A analyzes the quality of the approximation in two cases with low and high correlation. Section IV illustrates the quality of the approximation proposed for the calculation of the outage probability. Finally, Section V summarizes the contents of the paper.

B. Notation

Vectors and matrices are denoted by boldface lowercase and uppercase letter, respectively. The vector of absolute values of the components of $\boldsymbol{x}$ is denoted by $|\boldsymbol{x}|$. The product of the components of $\boldsymbol{x}$ is denoted by $\Pi(\boldsymbol{x})$. The vector of exponentials of the components of $\boldsymbol{x}$ is denoted by $\mathsf{e}^{\boldsymbol{x}}$. The notation $\mathrm{diag}(\boldsymbol{x})$ represents a diagonal matrix with the elements of the vector $\boldsymbol{x}$ on the main diagonal. $\mathcal{CN}(\boldsymbol{\mu}, \boldsymbol{\Sigma})$ represents the circularly-symmetric multivariate complex Gaussian distribution with mean vector $\boldsymbol{\mu}$ and covariance matrix $\boldsymbol{\Sigma}$.

II. System Model

Consider an RIS-aided communication system with single-antenna transmitter and receiver and a multi-element RIS. The received signal is represented by

$$Y = (H_d + \boldsymbol{g}^{\mathsf{H}}\boldsymbol{\Theta}\boldsymbol{h})X + Z. \tag{1}$$

Here, $H_d \sim \mathcal{CN}(0, \alpha)$ is the direct (transmitter-to-receiver) channel gain, $\boldsymbol{g} \sim \mathcal{CN}(\boldsymbol{0}, \boldsymbol{R})$ is the RIS-to-receiver vector gain, $\boldsymbol{\Theta}$ is the diagonal matrix of the RIS REs phase shifts, $\boldsymbol{h} \sim \mathcal{CN}(\boldsymbol{0}, \boldsymbol{R})$ is the transmitter-to-RIS vector gain, X is the transmitted signal, $Z \sim \mathcal{CN}(0, 1)$ is the additive noise, and Y is the received signal. The gains $H_d, \boldsymbol{g}, \boldsymbol{h}$ are independent. The covariance matrix $\boldsymbol{R}$, common for $\boldsymbol{g}$ and $\boldsymbol{h}$, is derived according to [1]:

$$(\boldsymbol{R})_{i,j} = \mathrm{sinc}(2\|\boldsymbol{u}_i - \boldsymbol{u}_j\|/\lambda), \tag{2}$$

where λ is the wavelength and $\boldsymbol{u}_i$ is the i-th RE location vector, for $i = 1, \ldots, N$. The function sinc is defined by $\mathrm{sinc}(x) \triangleq \sin(\pi x)/(\pi x)$. With perfect Channel State Information (CSI) at the RIS, the optimum choice for the diagonal element phases of the matrix $\boldsymbol{\Theta} = \mathrm{diag}(\mathsf{e}^{j\Theta_1}, \ldots, \mathsf{e}^{j\Theta_N})$ is

$$\Theta_i = \angle(H_d) + \angle(\boldsymbol{g})_i - \angle(\boldsymbol{h})_i. \tag{3}$$

Let the overall channel gain be:

$$\Gamma \triangleq H_d + \boldsymbol{g}^{\mathsf{H}}\boldsymbol{\Theta}\boldsymbol{h} \tag{4}$$

The resulting absolute value of the optimum overall channel gain is therefore:

$$|\Gamma_{\mathsf{opt}}| = |H_d| + \sum_{i=1}^{N} |(\boldsymbol{g})_i||(\boldsymbol{h})_i|. \tag{5}$$

In this expression we find the sum of multiple products of correlated Rayleigh envelopes, whose joint distribution is not known [7].

A. Outage Probability

The outage probability of a block fading channel can be obtained as the probability that the instance of the channel capacity depending on the channel gain is lower than a given target rate R. Assuming the RIS-aided communication channel follows the optimum model introduced above and considered in the literature [1], the outage probability is given by the following expression:

$$\begin{aligned} P_{\mathsf{out}} &= P(\log_2(1 + |\Gamma_{\mathsf{opt}}|^2\rho) < R) \\ &= P\left(|\Gamma_{\mathsf{opt}}| < \sqrt{\frac{2^R - 1}{\rho}}\right), \end{aligned} \tag{6}$$

where ρ is the reference SNR (corresponding to a unit-gain transmission system). The outage probability can be evaluated by using the Moment-Generating Function (MGF) of the absolute value of the channel amplitude gain, which is defined as:

$$\Phi_\Gamma(s) \triangleq \mathbb{E}\left[\mathsf{e}^{-s|\Gamma_{\mathsf{opt}}|}\right]. \tag{7}$$

The upper bound $u(x) \leq \mathsf{e}^{sx}$, valid for any $s \geq 0$, can be applied to the random variable

$$\Delta \triangleq |\Gamma_{\mathsf{opt}}| - \sqrt{\frac{2^R - 1}{\rho}}. \tag{8}$$

The following upper bound is obtained:

$$P_{\mathsf{out}} = P(\Delta < 0) = \mathbb{E}[u(-\Delta)] \leq \Phi_\Delta(s) = \mathbb{E}[\mathsf{e}^{-s\Delta}]. \tag{9}$$

Finally, the *Chernoff bound* is obtained by minimizing the previous upper bound:

$$P_{\mathsf{out}} \leq \min_{s \geq 0} \Phi_\Delta(s). \tag{10}$$

A more precise result is derived by using the Gauss-Chebyshev quadrature rule [9]. The starting point is the integral:

$$P_{\mathsf{out}} = \frac{1}{2\pi\mathrm{j}} \int_{c-\mathrm{j}\infty}^{c+\mathrm{j}\infty} \Phi_\Delta(s) \frac{ds}{s}, \tag{11}$$

where c is a positive real number in the Region of Convergence (ROC) of the MGF $\Phi_\Delta(s)$. Then, a Gauss-Chebyshev quadrature rule with ν nodes can be derived:

$$\begin{aligned} P_{\mathsf{out}} = \frac{1}{2\nu} \sum_{k=1}^{\nu} \{&\Re[\Phi_\Delta(c(1 + \mathrm{j}\tau_k))] \\ &+ \tau_k \Im[\Phi_\Delta(c(1 + \mathrm{j}\tau_k))]\} + E_\nu, \end{aligned} \tag{12}$$

where $\tau_k \triangleq \tan((k - 1/2)\pi/\nu)$ and $E_\nu \to 0$ as $\nu \to \infty$. Summarizing, the outage probability can be approximated by the Chernoff bound or by the Gauss-Chebyshev quadrature rule after the derivation of the MGF of $|\Gamma_{\mathsf{opt}}|$.

III. Moment-Generating Function

The MGF of $|\Gamma_{\mathsf{opt}}|$ is the product of two terms:

$$\Phi_\Gamma(s) = \Phi_d(s)\Phi_{\mathsf{RIS}}(s) \tag{13}$$

where

$$\Phi_d(s) \triangleq \mathbb{E}[\mathsf{e}^{-s|H_d|}] \tag{14}$$

$$\Phi_{\mathsf{RIS}}(s) \triangleq \mathbb{E}\left[\mathsf{e}^{-s\sum_{i=1}^{N} |(\boldsymbol{g})_i||(\boldsymbol{h})_i|}\right] \tag{15}$$

The first term can be calculated in closed form:

$$\Phi_d(s) = 1 - \sqrt{\pi\alpha}\, s\, \mathsf{e}^{\alpha s^2/4} Q\left(\sqrt{\frac{\alpha}{2}} s\right). \tag{16}$$

The second term can be calculated in closed form when the elements of $\boldsymbol{g}$ and $\boldsymbol{h}$ are uncorrelated.

Remark 1: The following integral is required for the calculation of the MGF in the uncorrelated case considered in this section and in the correlated case in the next subsection (defined for $a > 0, \Re(b) > -a$, and $m, n \in \mathbb{Z}_{\geq 0}$):

$$\begin{aligned}\mathcal{F}(a,b,m,n) &\triangleq \int_{\mathbb{R}_+^2} \mathrm{e}^{-a(x^2+y^2)-2bxy} 4x^{2m+1}y^{2n+1}dxdy \\ &= \frac{m!n!}{a^{m+n+2}}\,{}_2F_1\left(m+1, n+1; \frac{1}{2}; \frac{b^2}{a^2}\right) \\ &+ \frac{\pi(2m+1)!(2n+1)!}{2^{2m+2n+3}(m+1)!(n+1)!a^{m+n+3}b}\Bigg\{(a^2-b^2) \\ &\cdot {}_2F_1\left(m+\frac{3}{2}, n+\frac{3}{2}; -\frac{1}{2}; \frac{b^2}{a^2}\right) + (2(m+n+3)b^2 - a^2) \\ &\cdot {}_2F_1\left(m+\frac{3}{2}, n+\frac{3}{2}; \frac{1}{2}; \frac{b^2}{a^2}\right)\Bigg\}. \end{aligned} \tag{17}$$

The hypergeometric function ${}_2F_1(\alpha, \beta; \gamma; z)$ is defined by its series expansion in [10, 9.14]. Simplified expressions in special cases are:

$$\mathcal{F}(a,b,0,0) = \frac{a^2 - b^2 - b\sqrt{a^2-b^2}\arccos(b/a)}{(a^2-b^2)^2} \tag{18}$$

$$\mathcal{F}(a,a,0,0) = \frac{1}{3a^2} \tag{19}$$

$$\mathcal{F}(a,0,m,n) = \frac{m!n!}{a^{m+n+2}} \tag{20}$$

$$\begin{aligned}\mathcal{F}(a,a,m,n) = \frac{(m+n+1)!}{4a^{m+n+2}}\Bigg\{ \\ \frac{{}_2F_1(2(m+1), 2(m+n+2); 2m+3; -1)}{m+1} \\ + \frac{{}_2F_1(2(n+1), 2(m+n+2); 2n+3; -1)}{n+1}\Bigg\}\end{aligned} \tag{21}$$

■

Applying (18), $\Phi_{\mathsf{RIS}}(s)$ can be obtained as:

$$\begin{aligned}\Phi_{\mathsf{RIS}}(s) &= \left\{\int_{\mathbb{R}_+^2} \mathrm{e}^{-x^2-y^2-sxy} 4xydxdy\right\}^N \\ &= \left\{\mathcal{F}(1, s/2, 0, 0)\right\}^N \\ &= \left\{4\frac{4 - s^2 - s\sqrt{4-s^2}\arccos(s/2)}{(4-s^2)^2}\right\}^N \end{aligned} \tag{22}$$

Fig. 1 compares the MGF $\Phi_{RIS}(s)$ obtained analytically [eq. (22)] and by Monte-Carlo simulation with a variable number N of REs. The calculations are more difficult when the elements of $\boldsymbol{g}$ and $\boldsymbol{h}$ are correlated and this is an open problem except for some specific cases [7].

A. Correlated case

Define the phase vectors $\boldsymbol{\phi}_x, \boldsymbol{\phi}_y$ of the RIS gains $\boldsymbol{g}, \boldsymbol{h}$ and the corresponding diagonal matrices $\boldsymbol{\Phi}_x \triangleq \mathrm{diag}(\mathrm{e}^{\mathrm{j}\boldsymbol{\phi}_x})$, $\boldsymbol{\Phi}_y \triangleq \mathrm{diag}(\mathrm{e}^{\mathrm{j}\boldsymbol{\phi}_y})$. From the joint multivariate complex Gaussian distribution of $\boldsymbol{g}, \boldsymbol{h}$ in polar coordinates, the following

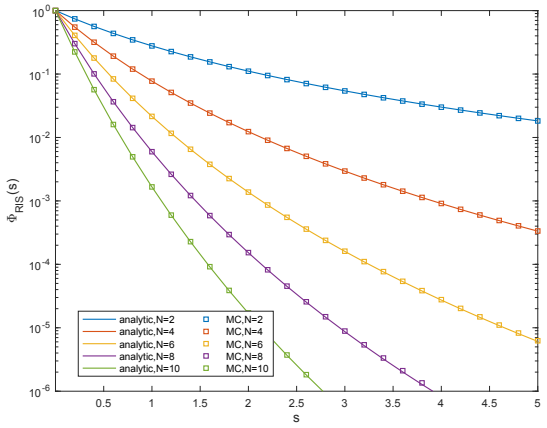

Fig. 1. Numerical validation of the MGF $\Phi_{\mathsf{RIS}}(s)$ from eq. (22).

expression of the MGF of the RIS component of $|\Gamma_{\mathsf{opt}}|$ can be written as follows:

$$\begin{aligned}\Phi_{\mathsf{RIS}}(s) = \frac{1}{\det(\pi\boldsymbol{R})^2}\int_{\mathbb{R}_+^{2N}}\int_{(0,2\pi)^{2N}} \Pi(\boldsymbol{x})\Pi(\boldsymbol{y}) \\ \mathrm{e}^{-\binom{\boldsymbol{x}}{\boldsymbol{y}}^{\mathsf{T}}\begin{pmatrix}\boldsymbol{\Phi}_x^*\boldsymbol{R}^{-1}\boldsymbol{\Phi}_x & (s/2)\boldsymbol{I}_N \\ (s/2)\boldsymbol{I}_N & \boldsymbol{\Phi}_y^*\boldsymbol{R}^{-1}\boldsymbol{\Phi}_y\end{pmatrix}\binom{\boldsymbol{x}}{\boldsymbol{y}}} d\boldsymbol{x}d\boldsymbol{y}d\boldsymbol{\phi}_x d\boldsymbol{\phi}_y\end{aligned} \tag{23}$$

A first step in the calculation of (23) is the integration of the phase variables. Consider the integral:

$$\mathcal{I}(\boldsymbol{x}) \triangleq \frac{1}{\det(\pi\boldsymbol{R})}\int_{(0,2\pi)^N} \mathrm{e}^{-\boldsymbol{x}^{\mathsf{T}}\boldsymbol{\Phi}_x^*\boldsymbol{R}^{-1}\boldsymbol{\Phi}_x\boldsymbol{x}} d\boldsymbol{\phi}_x. \tag{24}$$

Let $\boldsymbol{D} \triangleq \mathrm{diag}(\boldsymbol{R}^{-1}), \boldsymbol{\Delta} \triangleq \boldsymbol{R}^{-1} - \boldsymbol{D}$. Then, since diagonal matrices commute, $\boldsymbol{\Phi}_x^*\boldsymbol{D}\boldsymbol{\Phi}_x = \boldsymbol{D}$, and hence:

$$\mathcal{I}(\boldsymbol{x}) = \frac{1}{\det(\pi\boldsymbol{R})}\mathrm{e}^{-\boldsymbol{x}^{\mathsf{T}}\boldsymbol{D}\boldsymbol{x}}\int_{(0,2\pi)^N} \mathrm{e}^{-\boldsymbol{x}^{\mathsf{T}}\boldsymbol{\Phi}_x^*\boldsymbol{\Delta}\boldsymbol{\Phi}_x\boldsymbol{x}} d\boldsymbol{\phi}_x. \tag{25}$$

Following Miller's approach [8], the series expansion of $\exp(-\boldsymbol{x}^{\mathsf{T}}\boldsymbol{\Phi}_x^*\boldsymbol{\Delta}\boldsymbol{\Phi}_x\boldsymbol{x})$ can be evaluated. Since this series expansion is uniformly convergent with respect to $\boldsymbol{\phi}_x$, term-by-term integration can be applied and yields the following result:

$$\mathcal{I}(\boldsymbol{x}) = \frac{2^N}{\det(\boldsymbol{R})}\mathrm{e}^{-\boldsymbol{x}^{\mathsf{T}}\boldsymbol{D}\boldsymbol{x}}\sum_{k=0}^{\infty}\mathcal{P}_k(\boldsymbol{\Delta}, \boldsymbol{x}), \tag{26}$$

where

$$\mathcal{P}_k(\boldsymbol{\Delta}, \boldsymbol{x}) \triangleq \frac{(-1)^k}{k!(2\pi)^N}\int_{(0,2\pi)^N} (\boldsymbol{x}^{\mathsf{T}}\boldsymbol{\Phi}_x^*\boldsymbol{\Delta}\boldsymbol{\Phi}_x\boldsymbol{x})^k d\boldsymbol{\phi}_x. \tag{27}$$

Since $\boldsymbol{\Delta}$ is a Hermitian matrix with zero diagonal elements, the first values of $\mathcal{P}_k(\boldsymbol{\Delta}, \boldsymbol{x})$ are obtained as follows:

$$\mathcal{P}_0(\boldsymbol{\Delta}, \boldsymbol{x}) = 1 \tag{28}$$

$$\mathcal{P}_1(\boldsymbol{\Delta}, \boldsymbol{x}) = 0 \tag{29}$$

$$\mathcal{P}_2(\boldsymbol{\Delta}, \boldsymbol{x}) = \sum_{1\leq i<j\leq N} |(\boldsymbol{\Delta})_{i,j}|^2 x_i^2 x_j^2 \tag{30}$$

These polynomials are invariant with respect to joint permutations of the elements of the vector $\boldsymbol{x}$ and the rows and columns of the matrix $\boldsymbol{\Delta}$. In fact, if $\boldsymbol{\Pi}$ is an arbitrary permutation

matrix, the joint permutation can be implemented by the mappings $\boldsymbol{x} \mapsto \boldsymbol{\Pi x}, \boldsymbol{\Delta} \mapsto \boldsymbol{\Pi \Delta \Pi}^{\mathsf{T}}$. The mappings leave the integral invariant since:

1) Setting $\hat{\boldsymbol{\Phi}}_x = \boldsymbol{\Pi \Phi}_x \boldsymbol{\Pi}^{\mathsf{T}}$, we have:

$$(\boldsymbol{\Pi x})^{\mathsf{T}} \boldsymbol{\Phi}_x^* (\boldsymbol{\Pi \Delta \Pi}^{\mathsf{T}}) \boldsymbol{\Phi}_x (\boldsymbol{\Pi x}) = \boldsymbol{x}^{\mathsf{T}} \hat{\boldsymbol{\Phi}}_x^* \boldsymbol{\Delta} \hat{\boldsymbol{\Phi}}_x \boldsymbol{x}. \quad (31)$$

2) The negative exponential of this quadratic form is integrated over the phase space $\boldsymbol{\phi}_x \in (0, 2\pi)^N$.

Next, the integration over $\boldsymbol{x}$ is simplified by the fact that the exponential $\mathrm{e}^{-\boldsymbol{x}^{\mathsf{T}} \boldsymbol{D} \boldsymbol{x}}$ factors into the product $\prod_{i=1}^N \mathrm{e}^{-(\boldsymbol{D})_{ii} x_i^2}$. Then, the integral can be calculated as follows:

$$\Phi_{\mathsf{RIS}}(s) = \frac{1}{\det(\boldsymbol{R})^2} \int_{\mathbb{R}_+^{2N}} \prod_{i=1}^N \mathrm{e}^{-(\boldsymbol{D})_{ii}(x_i^2+y_i^2) - s x_i y_i} \cdot \sum_{k=0}^{\infty} \mathcal{P}_k(\boldsymbol{\Delta}, \boldsymbol{x}) \sum_{k'=0}^{\infty} \mathcal{P}_{k'}(\boldsymbol{\Delta}, \boldsymbol{y}) \Pi(2\boldsymbol{x}) \Pi(2\boldsymbol{y}) d\boldsymbol{x} d\boldsymbol{y}. \quad (32)$$

A second-order approximation of this results is given by:

$$\Phi_{\mathsf{RIS}}(s) \approx \frac{1}{\det(\boldsymbol{R})^2} \int_{\mathbb{R}_+^{2N}} \prod_{i=1}^N \mathrm{e}^{-(\boldsymbol{D})_{ii}(x_i^2+y_i^2) - s x_i y_i} \cdot \{1 + \mathcal{P}_2(\boldsymbol{\Delta}, \boldsymbol{x}) + \mathcal{P}_2(\boldsymbol{\Delta}, \boldsymbol{y})\} \Pi(2\boldsymbol{x}) \Pi(2\boldsymbol{y}) d\boldsymbol{x} d\boldsymbol{y}. \quad (33)$$

Finally, setting

$$\hat{\mathcal{F}}_{i,m,n}(s) \triangleq \mathcal{F}((\boldsymbol{D})_{ii}, s/2, m, n), \quad (34)$$

yields the following second-order approximation: $\Phi_{\mathsf{RIS}}(s) \approx$

$$\frac{\prod_{i=1}^N \hat{\mathcal{F}}_{i,0,0}(s)}{\det(\boldsymbol{R})^2} \left\{ 1 + 2 \sum_{i<j} |(\boldsymbol{\Delta})_{i,j}|^2 \frac{\hat{\mathcal{F}}_{i,1,0}(s)}{\hat{\mathcal{F}}_{i,0,0}(s)} \frac{\hat{\mathcal{F}}_{j,1,0}(s)}{\hat{\mathcal{F}}_{j,0,0}(s)} \right\}. \quad (35)$$

B. Validation

To validate the quality of this approach, the following cases are considered.

- 2×2 rectangular RIS;
- 4×2 rectangular RIS;
- 4×4 rectangular RIS.

Figures 2 and 3 demonstrate the accuracy of the second-order approximation of the MGF, $\Phi_{\mathsf{RIS}}(s)$, across the positive real line for various rectangular RIS configurations, considering antenna spacings of $h = \lambda$ and $h = \lambda/2$, respectively. The approximation is more accurate with $h = \lambda$ compared to $h = \lambda/2$, as larger antenna spacing results in lower correlation.

IV. Application: Outage Probability

This section considers the evaluation of the outage probability based on the approach developed in Section II-A.

Figs. 4 to 6 illustrate the outage probability corresponding to normalized antenna spacings $h/\lambda = 0.5, 1$, and 10, respectively, for the RIS-aided wireless links whose parameters are specified in the figure caption. The number of nodes used for the Gauss-Chebyshev quadrature rule is $\nu = 256$. Fig. 4 shows that the proposed approach yields very accurate results up to the 4×2 RIS, acceptable in the 4×4 case, and bad in the

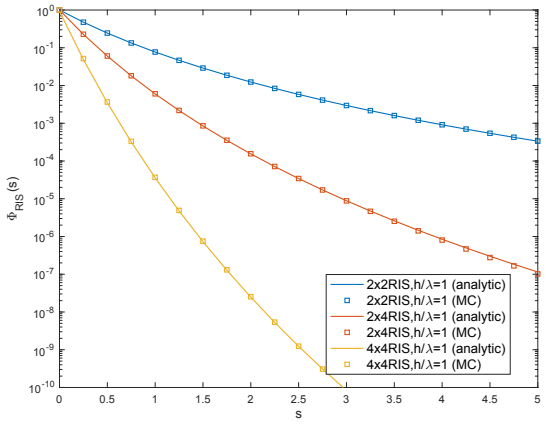

Fig. 2. Plot of the MGF $\Phi_{\mathsf{RIS}}(s)$ for $h = \lambda$ and several rectangular RISs.

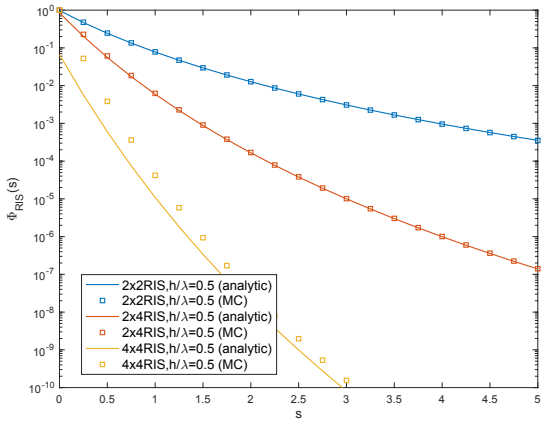

Fig. 3. Same as Fig. 2 but $h = \lambda/2$.

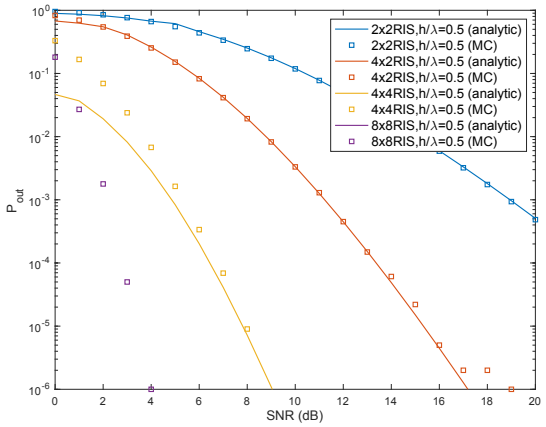

Fig. 4. Outage probability for several rectangular RIS with target rates $R = 5$ bit/s/Hz (2×2 RIS), $R = 6$ bit/s/Hz (4×2 RIS), $R = 7$ bit/s/Hz (4×4 RIS), and $R = 11$ bit/s/Hz (8×8 RIS), no direct signal propagation, and antenna spacing $h = \lambda/2$. Monte-Carlo simulation results (based on 10^6 samples) are also reported for comparison.

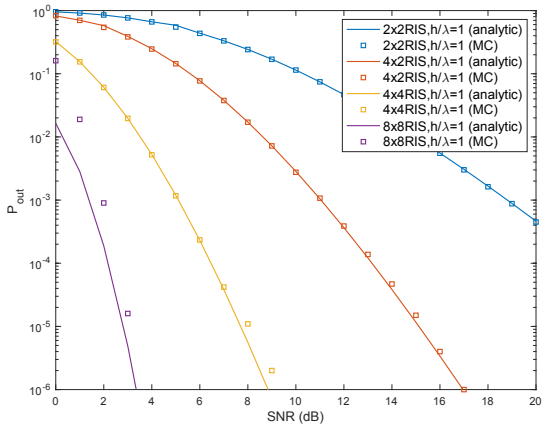

Fig. 5. Same as Fig. 4 but with antenna spacing $h = \lambda$.

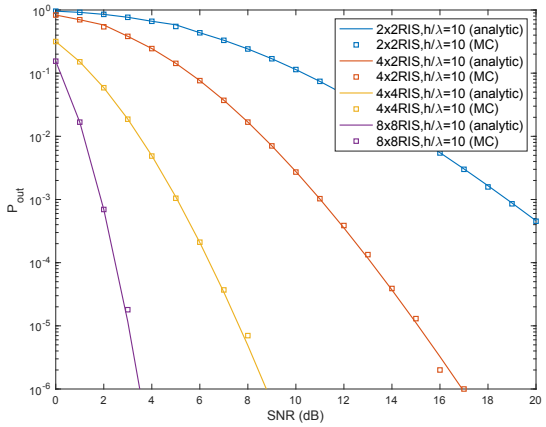

Fig. 6. Same as Fig. 4 but with $h = 10\lambda$.

8×8 case. Increasing the antenna spacing to $h = \lambda$ yields the results in Fig. 5, which show that the approximation is still limited in the 8×8 RIS case. With $h = 10\lambda$, the approximation is excellent in all cases considered (Fig. 6). The increased accuracy with larger values of h depends on the fact that correlation diminishes as the antenna spacing increases. The difference in outage probability corresponding to $h/\lambda = 1/2$ and 1 is only marignally noticeable in the 2×2 RIS scenario.

A. Applicability of the results

The literature suggests that typical RIS structures consist of panels with an approximate area of $1\,\mathrm{m}^2$, containing up to 25 elements arranged in a rectangular array (as a rough estimate). This corresponds to an antenna spacing of 20 cm. For a carrier frequency of 30 GHz, this spacing translates to $h = 10\lambda$. Consequently, the preceding results are highly relevant within this range of normalized spacing factors.

V. Conclusions

In this paper, we introduced a second-order approximation of the Moment-Generating Function (MGF) for the sum of the product of correlated Rayleigh envelopes (a problem well-known in the literature [7], [8]), which was applied to evaluate the outage probability for both uncorrelated and correlated Reconfigurable Intelligent Surfaces (RIS). The primary contributions include the derivation of the MGF and its use in outage probability evaluation across different scenarios. We also assessed the accuracy of the proposed approximation under two distinct correlation conditions, demonstrating its reliability in providing outage probability estimates. The results highlight the effectiveness of the second-order approximation as a practical tool for evaluating the outage probability in RIS-based systems, particularly in correlated environments. The findings offer valuable insights for future research and practical applications of RIS in wireless communication systems, particularly in optimizing performance in the presence of varying correlation conditions.

Future research could explore higher-order approximations of the MGF, enabling the technique to be applied to scenarios where the current approximation lacks sufficient accuracy.

References

[1] E. Björnson and L. Sanguinetti, "Rayleigh fading modeling and channel hardening for reconfigurable intelligent surfaces," *IEEE Wireless Communications Letters*, vol. 10, no. 4, pp. 830–834, 2021.

[2] M. Di Renzo, A. Zappone, M. Debbah, M.-S. Alouini, C. Yuen, J. de Rosny, and S. Tretyakov, "Smart radio environments empowered by reconfigurable intelligent surfaces: How it works, state of research, and the road ahead," *IEEE Journal on Selected Areas in Communications*, vol. 38, no. 11, pp. 2450–2525, 2020.

[3] O. Tsilipakos *et al.*, "Toward intelligent metasurfaces: The progress from globally tunable metasurfaces to software-defined metasurfaces with an embedded network of controllers," *Advanced Optical Materials*, vol. 8, no. 17, p. 2000783, 2020.

[4] K. B. Letaief, W. Chen, Y. Shi, J. Zhang, and Y.-J. A. Zhang, "The roadmap to 6G: Ai empowered wireless networks," *IEEE Communications Magazine*, vol. 57, no. 8, pp. 84–90, 2019.

[5] Y. Liu, X. Liu, X. Mu, T. Hou, J. Xu, M. Di Renzo, and N. Al-Dhahir, "Reconfigurable intelligent surfaces: Principles and opportunities," *IEEE Communications Surveys & Tutorials*, vol. 23, no. 3, pp. 1546–1577, third quarter 2021.

[6] S. Rengarajan and Y. Rahmat-Samii, "The field equivalence principle: illustration of the establishment of the non-intuitive null fields," *IEEE Antennas and Propagation Magazine*, vol. 42, no. 4, pp. 122–128, 2000.

[7] R. Mallik, "On multivariate rayleigh and exponential distributions," *IEEE Transactions on Information Theory*, vol. 49, no. 6, pp. 1499–1515, 2003.

[8] K. Miller and R. Bernstein, "An analysis of coherent integration and its application to signal detection," *IRE Transactions on Information Theory*, vol. 3, no. 4, pp. 237–248, December 1957.

[9] G. Taricco and E. Biglieri, "Exact pairwise error probability of space-time codes," *IEEE Transactions on Information Theory*, vol. 48, no. 2, pp. 510–513, 2002.

[10] I. Gradshteyn and I. Ryzhik, *Table of Integrals, Series, and Products*. Elsevier Science, 2014.